2.B: 2.L

Nuclear Physics **55** (1964) 613—642;

ANGULAR CORRELATION STUDIES OF NUCLEAR POLARIZATION FOLLOWING INELASTIC SCATTERING OF ALPHA PARTICLES FROM C^{12} AND Mg^{24}

W. W. EIDSON, J. G. CRAMER, Jr., D. E. BLATCHLEY and R. D. BENT

Department of Physics, Indiana University, Bloomington, Indiana †

Received 7 January 1964

Abstract: Alpha-gamma angular correlations have been measured at 73 scattering angles in the reaction plane for the reaction $C^{12}(\alpha, \alpha'\gamma_{4.43})$ and at 40 scattering angles for the reaction $Mg^{24}(\alpha, \alpha'\gamma_{1.37})$. The correlation functions were determined at each alpha-particle scattering angle by measuring the coincidence gamma-ray yield for at least 11 different gamma-ray detection angles. All of the particles in both reactions except the excited nuclei and the gamma rays are spinless, greatly simplifying interpretation of the correlation data. These data have been analysed in terms of the polarization of the excited nucleus, and show the presence of curious and distinctive behaviour in the functional dependence of the polarization parameters on scattering angle for both reactions studied. These results are compared with the predictions of reaction theories and show strong disagreement with semi-classical, plane-wave, and adiabatic theory predictions, while giving at least qualitative agreement with DWBA calculations. Predictions of compound nucleus theory are investigated, and the relevance of this type of measurement to the investigation of reaction mechanisms and their interference effects is discussed.

E

NUCLEAR REACTION C^{12}, $Mg^{24}(\alpha, \alpha'\gamma)$, $E_\alpha = 22.5$ MeV; measured $\sigma(\theta)$, α-, γ-spectra, $\alpha'\gamma(\theta)$. C^{12}, Mg^{24} deduced polarization parameters. Natural targets.

1. Introduction

Experimental investigations of interactions of nuclei with medium-energy alpha particles have been confined almost exclusively to the measurement of elastic and inelastic differential cross sections, and a wealth of information now exists from such measurements. However, as discussed in the conclusion of the preceding paper [1]), these cross sections reflect only certain details of the nuclear process under investigation,while other equally important details are completely undetermined by simple cross section measurements.

This arises from the fact that the set of scattering amplitudes T_{jm} which provide the quantum mechanical description of the observable features of the inelastic scattering process appear in the cross section only in a sum of absolute squares, i.e. $d\sigma/d\Omega = \sum_m |T_{jm}|^2$. Thus the relative phases and relative magnitudes of the scattering amplitudes are averaged out and have no effect on the differential cross section and, consequently, cannot be studied by means of cross section measurements.

These quantities appear directly in the polarization of the excited nucleus following inelastic scattering from even nuclei. The preceding paper has described methods by which this nuclear polarization can be derived from the results of alpha-gamma

† This work was supported by the National Science Foundation.

angular correlation measurements [1]). Since the nuclear polarization, like the cross section, will generally vary with scattering angle, these measurements must be performed over a range of angles to determine the angular dependence of the polarization, and thus represent a time consuming though rewarding experimental investigation.

The purpose of this paper is to present the experimental results of such alpha-gamma correlation measurements performed on the reactions $C^{12}(\alpha, \alpha'\gamma)(Q = -4.43$ MeV) and $Mg^{24}(\alpha, \alpha'\gamma)(Q = -1.37$ MeV) and to discuss these results and their bearing on the polarization of the excited nucleus, the scattering amplitudes of the reaction process, and on current theoretical treatments of such reactions. Preliminary discussions of this work have been presented elsewhere. [2, 3])

The correlation function $W(\theta, \phi; \phi_{\alpha'})$, as measured in these experiments, represents the probability of emission of a gamma ray in a direction specified by the polar and azimuthal angles θ and ϕ when an alpha particle is inelastically scattered at an angle $\phi_{\alpha'}$. Here the angles are measured in a spherical polar coordinate system with the x-axis along the beam direction and the z-axis perpendicular to the plane of the reaction. The functional form of the correlation function has been treated extensively in the preceding paper [1]); it is a consequence of the angular momentum and symmetry properties of the reaction, and of the nuclear polarization produced by the inelastic scattering reaction.

When the excited nucleus has two units of angular momentum, as is the case in the present measurements, the correlation function has a particularly simple form in the reaction plane,

$$W(\tfrac{1}{2}\pi, \phi) = A + B \sin^2 2(\phi - \phi_0). \tag{1}$$

Although this form has sometimes mistakenly been associated with the direct reaction process, it is actually quite general and not dependent on the details of the reaction except in the values of the parameters A, B, and ϕ_0. However, by studying the behaviour of the free parameters A/B and ϕ_0, or the equivalent nuclear polarization parameters a_2 and δ_2 [1]), as functions of scattering angle, one can begin detailed study of the mechanism of the reaction.

The angular correlation data which will be presented below has been analysed in terms of the parameters a_2 and δ_2, which describe the polarization of the excited nucleus. To provide continuity with other work, [2, 4–6]) however, these data will also be analysed in terms of the symmetry angle ϕ_0.

2. Apparatus and Procedures

Self-supporting targets of natural carbon (1.5 mg/cm^2) and magnesium (2 mg/cm^2) were bombarded with 22.5 MeV alpha particles from the Indiana University cyclotron. Fig .1 shows the experimental area in which the measurements were made. The targets and the particle detector, a 1 cm^2 diffused-junction semiconductor detector, were located within a small 20 cm diameter scattering chamber. The gamma ray

detector was a 7.6 × 7.6 cm NaI(Tl) crystal integrally mounted on a DuMont 6363 photomultiplier tube. The gamma-ray detector assembly was mounted directly outside the scattering chamber on a radial dolly constrained to move concentrically in the reaction plane about the centre of the target. A detailed description of the physical arrangement which was employed can be found elsewhere. [7,8])

Pulses from the charged-particle detector were displayed on a 100-channel pulse-height analyser which was gated by conventional fast-slow coincidence circuitry. The

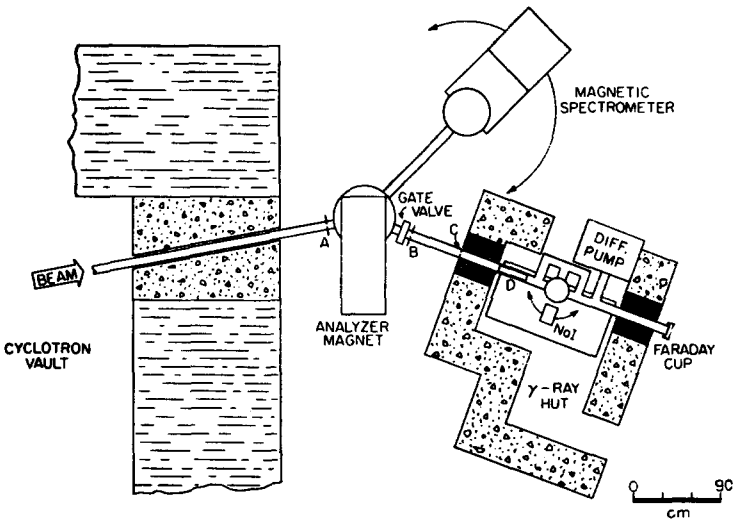

Fig. 1. Diagramme of experimental area. Beam emerging from cyclotron vault is deflected and analysed by 20° magnet and defined by slits at positions A, B, C and D, before entering the angular correlation chamber indicated by the small circle. Differential cross sections were measured in the larger scattering chamber attached to the magnetic spectrometer above.

resolving time used (2τ = 30nsec) was small enough to reject chance events in which the alpha particle and gamma ray were produced by different beam pulses of the cyclotron. A differential window was adjusted so that gating pulses were generated only by gamma-ray pulse-heights in the range 3.5 to 4.5 MeV for the C^{12} correlations and 1.0 to 1.5 MeV for the Mg^{24} correlations.

In an experiment of this type, the true-to-chance ratio is strongly dependent on the beam intensity. Because of the pulsed character of the cyclotron beam, it was necessary to limit the average beam current to between 0.02 and 0.003 microamperes. This current provided a true-to-chance ratio of between 10 and 100, depending on the relative intensities of the alpha particles and gamma rays. The chance counts were determined by measuring the ratio of counts in the elastic peak to those in the inelastic peak in the coincidence-gated alpha-particle energy spectrum and comparing this ratio to the analogous ratio in the ungated alpha spectrum. All correlation data presented below have been corrected for chance in this manner. A discussion of the electronics and shielding used in these measurements is given elsewhere. [7,8])

For most of the coincidence measurements, the particle detector was collimated to a 1.5° half-acceptance angle. In regions of alpha-particle scattering angle where the symmetry angle ϕ_0 of the correlation function was observed to shift rapidly, the correlation functions were remeasured with a particle-detector half-acceptance angle of 0.5°. The gamma-ray detector subtended a half-acceptance angle of 13° for all measurements.

Data were recorded by fixing the particle detector at a desired scattering angle and then systematically varying the gamma-ray detection angle in the reaction plane in 10° steps from 40° to 140°, as measured with respect to the beam direction but on the opposite side of the beam from the particle detector. Measurements were generally repeated at several of the gamma-ray angles for the purposes of checking and improving statistics. Since it was necessary to locate the Faraday cup approximately 7 feet from the target in order to reduce the gamma-ray background from 22.5 MeV alpha particles stopping in the cup, accurate integration of the beam was not feasible. However, only relative intensities are needed from the correlation measurements to determine the nuclear polarization, so this problem was not considered serious. Coincidence measurements taken at the same alpha-particle scattering angle were normalized by monitoring the elastic counting rate at that angle. This method was found to provide quite reproducible data, independent of beam intensity fluctuations and target thickness variations.

After subtraction of the chance counts the data were analysed using a least-squares fitting programme for the Indiana University IBM 709 computer. The observed correlation functions were fitted by an exact least-squares method [9]) to a function of the form

$$W_2(\tfrac{1}{2}\pi, \phi) = A_1 + A_2' \cos 4\phi + A_3' \sin 4\phi. \tag{2}$$

The rather large angular aperture of the gamma-ray detector (13° half angle) has the effect of averaging and smoothing the observed correlation function, and this effect is more pronounced in fast variations than in slow ones. Therefore, the experimental coefficients A_2' and A_3' must be corrected for this effect to obtain the "true" coefficients A_2 and A_3. Since an isotropic distribution is unaffected by smoothing, the isotropic coefficient A_1 needs no correction.

The correction of angular resolution distortion in angular correlation measurements has received some attention in the literature. [10, 11]) The correction of correlation measurements of the type presented here, however, involve a somewhat different problem than that usually treated, because the presence of a beam direction asymmetrizes the problem, and because the angular dependence of the correlation function out of the reaction plane has not been measured and is not known.

The method which was used here is a modification of that originally suggested by Rose [10]) for the correction of γ-γ correlation measurements. It involves numerical integration of the angular dependence of the correlation function (in this case cos 4ϕ) over the angular aperture and geometrical efficiency of the gamma-ray detector. This

procedure produces a multiplicative correction factor K which is given by the relation

$$K = \left(2\pi \int_0^{\gamma} E(\beta) \sin\beta \, \mathrm{d}\beta\right) \Big/ \left(\int_0^{\gamma}\int_0^{2\pi} \cos 4\alpha \, E(\beta) \sin\beta \, \mathrm{d}\phi \, \mathrm{d}\beta\right), \tag{3}$$

where $E(\beta) = (1-\exp(-\tau X(\beta)))$, $\alpha = \tan^{-1}(\tan\beta\cos\phi)$, and γ and τ are as defined by Rose [10]). Since there is a misprint in this reference in giving the relation for $X(\beta)$, we note that it is defined as

$$X(\beta) = t\sec\beta \; (0 \leqq \beta \leqq \beta'), \qquad X(\beta) = r\csc\beta - h\sec\beta \; (\beta' \leqq \beta \leqq \gamma),$$

where β', r, h, and t are also as given by Rose [10]). The true correlation function is then

$$W_2(\tfrac{1}{2}\pi, \phi) = A_1 + K(A_2' \cos 4\phi + A_3' \sin 4\phi) = A_1 + A_2 \cos 4\phi + A_3 \sin 4\phi. \tag{4}$$

Numerical evaluation of the correction factor K on the Indiana University IBM 709 computer gave the values $K(C^{12}) = 1.1490$ and $K(Mg^{24}) = 1.1542$, assuming a 7.6×7.6 cm NaI crystal at a distance of 12.9 cm from the centre of the target and including the absorption coefficient τ of NaI at the appropriate gamma ray energies.

The calculation described above includes the implicit assumption that the correlation function is constant as a function of the polar angle θ for a certain angular distance (13°) above and below the reaction plane. A more exact calculation requires a knowledge of the behaviour of the correlation function out of the reaction plane. However, a calculation which assumed a behaviour for the correlation function based on eq. (9) of the previous paper [1]) and which used the method of Rose *et al* [11]) to evaluate the correction factor exactly, agreed with the results of the calculation described above to better than 0.1 %.

The corrected coefficients A_1, A_2, and A_3 obtained from the fitting procedure were converted to the parameters a_2 and δ_2, which characterize the polarization of the excited nucleus following the inelastic scattering [1]). These polarization parameters are related to the A coefficients by

$$\begin{aligned} \delta_2 &= \arctan(A_3/A_2), \\ a_2 &= X^{\frac{1}{2}} - (X-1)^{\frac{1}{2}}, \qquad \text{where } X = A_1^2/(A_2^2+A_3^2) \\ &= 0, \text{ when } A_2 = A_3 = 0. \end{aligned} \tag{5}$$

In terms of these polarization parameters, the correlation function is

$$\begin{aligned} W(\tfrac{1}{2}\pi, \phi) &= (1-a_2)^2 + 4a_2 \sin^2 2(\phi - \tfrac{1}{4}\delta_2) \\ &= A + B\sin^2 2(\phi - \phi_0), \end{aligned} \tag{6}$$

the latter form being that given by eq. (1). Thus it is apparent that the symmetry angle ϕ_0 is given by $\delta_2 = 4\phi_0$. The symmetry angle is plotted as a function of the scattering angle for direct comparison with other work [2, 4-6]) (see fig. 8)

Since the data from which the polarization parameters are derived are subject to experimental errors and uncertainties, these uncertainties will be reflected in the para-

meters themselves and must be taken into account during analysis. The errors in the parameters were calculated under the assumptions that the errors Δy_i in the data points y_i are independent of each other, are non-systematic, and are purely statistical, so that $\Delta y_i = \pm(y_i)^{\frac{1}{2}}$. The RMS error Δp_j in a given parameter p_j was calculated from the relation

$$\Delta p_j = \left[\sum_i \left(\frac{\partial p_j}{\partial y_i} \right)^2 y_i \right]^{\frac{1}{2}}. \tag{7}$$

The partial derivative $\partial p_j/\partial y_i$ was calculated by "regression" through the various steps in the least-squares fitting procedure from the polarization parameters p_j to the raw data points y_i, performing a sum over the partial derivatives of the appropriate intermediate variables at each step of the regression. Thus the single derivative in (7) is actually a derivative chain, and

$$\Delta p_j = \{ \sum_i [\sum_k (\partial p_j/\partial A_k) \sum (\partial A_k/\ldots) \ldots \sum_m (\ldots/\partial Z_m)(\partial Z_m/\partial y_i)]^2 y_i \}^{\frac{1}{2}}. \tag{8}$$

After the correlation data points were fitted, the correlation function was reconstructed from the derived parameters and a χ-squared test applied to determine the quality of the fit. The Lexis coefficient [12]), which is the χ-squared value divided by the number of data points in the fit, will be tabulated along with the data as a measure of the quality of the fit. A Lexis coefficient of zero represents a perfect fit, a value of 1 is within statistics, and a value of less than 5 represents a fairly good fit.

In addition to the statistical errors present in the data points, there was some necessary uncertainty in the measurement of the particle and gamma-ray detection angles. The absolute particle detection angles are estimated to be accurate to within $\pm 2°$, the gamma-ray detection angles to within $\pm 3°$, and the relative error in both angular measurements is estimated to be less than $\pm 1°$.

To complement the angular correlation measurements described above, differential cross sections were measured for elastic and inelastic scattering of alpha particles from carbon† and magnesium [13]). These measurements were performed in a larger (40.6 cm diameter) precision scattering chamber. The scattered particles were detected with a surface-barrier semiconductor detector, and the beam energy was monitored simultaneously with a 180° double-focussing magnetic spectrometer. The beam energy was established as 22.48 ± 0.05 MeV at all times during the measurement. The total absolute error on the differential cross-sections was estimated to be less than 30 %.

3. Experimental Results

Fig. 2 shows a typical particle spectrum obtained by observing charged-particle reaction products from the bombardment of a 1.5 mg/cm^2 carbon target with 22.5 MeV alpha particles. The diffused-junction detector was located at a laboratory scat-

† Differential cross sections for $C^{12}+\alpha$ are used with the permission of Dr. R. A. Atneosen, who performed the measurements.

tering angle of 22 degrees and was collimated to a solid angle of 0.3 % of the total sphere. The broadening of the peaks was due mainly to target thickness and kinematical energy spread over the large detector aperture. Both of these were necessary in

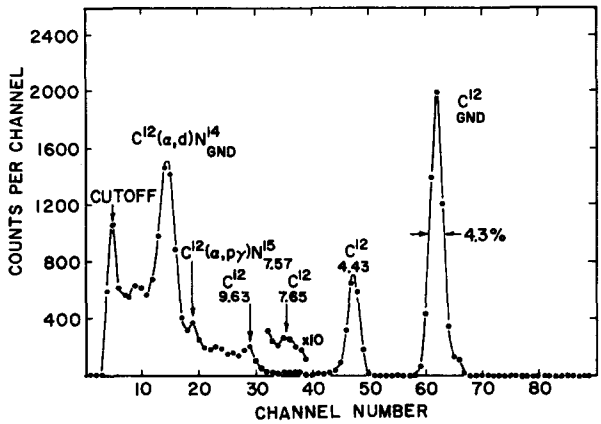

Fig. 2. Typical particle spectrum from the bombardment of natural carbon with 22.5 MeV alpha particles, measured at $\phi_{\alpha'}$(lab) = 22.0°. Peaks corresponding to elastic and inelastic scattering of alpha particles are labelled with the excitation energy of the state excited.

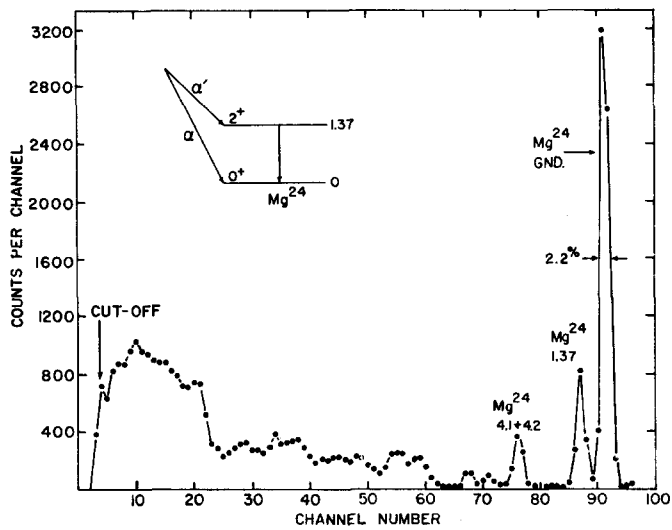

Fig. 3. Typical particle spectrum from the bombardment of natural magnesium with 22.5 MeV alpha particles, measured at $\phi_{\alpha'}$(lab) = 22.5°.

order to obtain reasonable coincidence efficiency. However, it is clear that the inelastic alpha-particle group leading to the first excited state ($Q = -4.43$ MeV) of C^{12} was clearly resolvable. Fig. 3 shows a similar particle spectrum obtained from the bombardment of a natural magnesium target 2.0 mg/cm^2 with 22.5 MeV alpha particles.

Detector collimation was narrowed to about 0.15 % of the total sphere for this and all the coincidence measurements of $Mg^{24}(\alpha, \alpha'\gamma)Mg^{24}$. Again, it is clear that the inelastic alpha-group particle leading to the first excited state (Q = 1.37 MeV) of

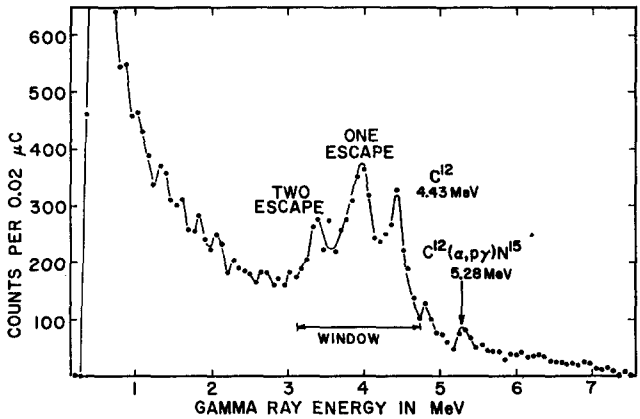

Fig. 4. Typical NaI(Tl) scintillation spectrum of gamma rays produced when natural carbon is bombarded with 22.5 MeV alpha particles. The window or energy interval of gamma rays accepted in the coincidence measurement is indicated.

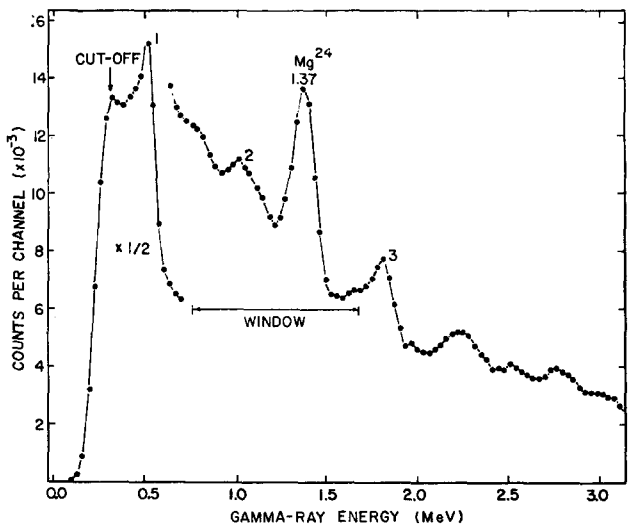

Fig. 5. Typical NaI(Tl) scintillation spectrum of gamma rays produced when natural magnesium is bombarded with 22.5 MeV alpha particles. Peaks labelled numerically are (1) 0.511 MeV positon annihilation radiation, (2) 1.10 MeV gamma rays produced by decay from the second to the first excited state of Mg^{26}, and (3) gamma rays from the decay of the first excited state of Mg^{26}. The window or interval of gamma rays accepted in the coincidence measurement is indicated.

Mg^{24} was clearly resolvable for the coincidence measurements. The spectra used for the angular distribution calculations were recorded with much narrower collimation

(0.01 % of the total sphere) and much thinner targets (0.2 mg/cm^2) with better resolution.

Figs. 4 and 5 respectively, show gamma-ray spectra (singles spectra with no coincidence requirement) resulting from bombardment of natural carbon and magnesium targets with 22.5 MeV alpha particles. Gamma-ray counting rates of 50 000 to 100 000 counts per second were used for the coincidence measurements, but the spectra shown here were recorded at about 10 000 counts per second so as not to jam the multichannel analyser. The de-excitation gamma-rays from the first excited states of Mg^{24} and C^{12} are clearly discernable above background even in these singles

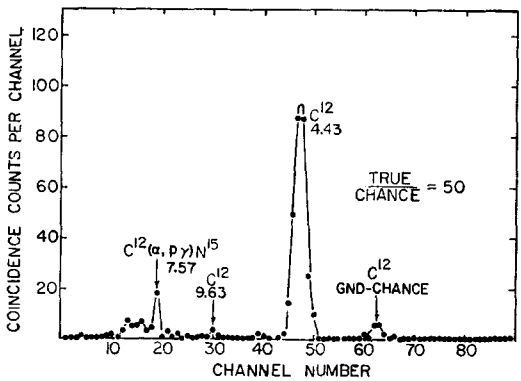

Fig. 6. Typical spectrum of particles measured in coincidence with 3.5-4.5 MeV gamma rays for the $C^{12}(\alpha, \alpha'\gamma)$ reaction. All peaks shown except those labelled C^{12} 4.43 and $C^{12}(\alpha, p\gamma)N^{15}$ are the result of chance coincidences. One spectrum of this type was measured to obtain each point on each correlation function studied.

spectra. The differential windows used for pulse-height selection are indicated in the figures. (In fig. 4, the 5.28 MeV peak labelled $C^{12}(\alpha, p\gamma)N^{15}$ was assigned in previous work [8]). Numbered peaks in fig. 5 are assigned in the caption of that figure. Spectroscopic measurements were made by setting the differential window on the appropriate inelastic alpha-particle group which confirmed the assignments indicated in the figures).

Fig. 6 is a charged-particle spectrum obtained from the bombardment of the carbon target with 22.5 MeV alpha particles and recorded in coincidence with 4.43 MeV gamma rays as indicated by the differential window position in fig. 4. The gamma-ray detector was located at an angle of 90° with respect to the beam direction. It is noticed that the inelastic alpha-particle group leading to the 4.43 MeV state of C^{12} is in coincidence with 4.43 MeV gamma rays with an observed true-to-chance ratio of 50. All other groups observed represent chance except for the N^{15} proton group [8]). Comparison of figs. 4 and 6 provides a simple direct method of estimating chance (see section 2 above); the spectrum shown is a typical one, as the true-to-chance ratio was observed to be as high as several hundred for high-yield correlation angles. Similar data was

obtained for the magnesium target. Each point of each correlation pattern was obtained from a spectrum like fig. 6, and each was corrected for chance in the manner described.

Fig. 7 shows chance-subtracted $C^{12}(\alpha, \alpha'\gamma)C^{12}$ correlation data taken at three different alpha-particle scattering angles. These (and all other) correlation patterns were

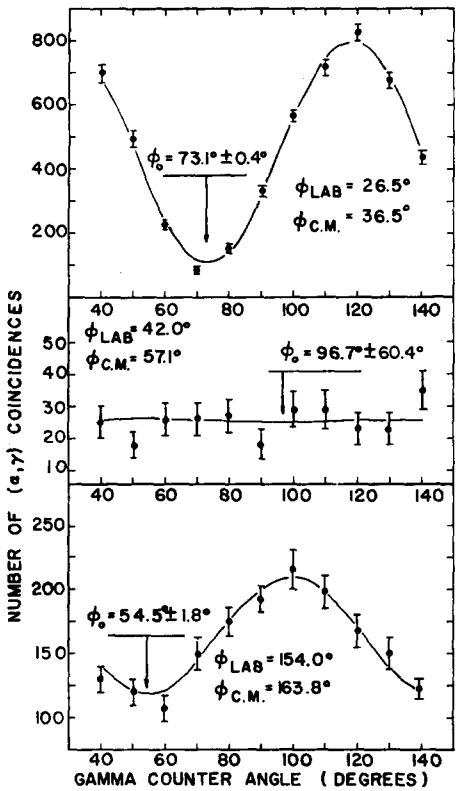

Fig. 7. Typical correlation functions for the $C^{12}(\alpha, \alpha'\gamma)$ reaction. Points have been corrected for chance. Error bars shown reflect only statistical errors arising from counting statistics. Lines through the points are least squares fits to the functional form given by eq. (2).

measured by fixing the alpha-particle detection angle and counting the number of inelastic alpha particles observed above chance for successive locations of the gamma-ray detector from 40° to 140° with respect to the beam direction. The error bars on the data points are statistical and do not include the extrinsic errors discussed in sect. 2 of this paper. For each correlation, the solid lines represent best least-squares fits of the function $A+B\sin^2 2(\phi-\phi_0)$ to the correlation data. The data shown were corrected for chance, but neither the data nor the fits were corrected for the solid angle of the gamma-ray detector for these sample correlation patterns. The centre correlation pattern in fig. 7 (lab. scattering angle 42.0°) is statistically almost meaningless,

TABLE 1
$C^{12}(\alpha, \alpha'\gamma)$ angular correlation results

$\phi_{\alpha'}$(lab) (degrees)	$\phi_{\alpha'}$(c.m.) (degrees)	δ_2 (degrees)	a_2	Lexis coeff.
11.00	15.263	220.6± 6.1	0.378±0.050	9.969
13.00	18.028	117.6± 8.9	0.135±0.022	0.565
14.00	19.408	155.9±16.7	0.091±0.029	3.255
15.00	20.787	92.3± 4.4	0.229±0.024	3.828
17.00	23.540	80.3± 3.1	0.244±0.018	3.328
19.00	26.287	82.6± 2.8	0.357±0.034	1.572
21.50	29.709	73.4± 2.0	0.368±0.026	1.819
24.00	33.117	66.4± 1.5	0.549±0.051	0.669
26.50	36.511	67.8± 1.8	0.628±0.094	1.077
29.00	39.887	64.1± 1.5	0.833±0.137	0.845
31.50	43.245	66.8± 1.6	1.000±0.150	1.570
34.00	46.583	63.9± 1.6	0.543±0.039	3.415
36.50	49.900	61.1± 2.3	0.551±0.078	1.298
39.00	53.192	47.6± 3.0	0.364±0.029	3.844
41.00	55.809	31.4± 5.7	0.251±0.048	2.210
42.00	57.111	333. ±241.	0.013±0.499	0.836
42.50	57.760	23.4±14.3	0.091±0.028	3.625
43.00	58.408	133.9±15.5	0.188±0.063	0.491
44.00	59.702	133.3± 5.1	0.232±0.035	1.038
45.00	60.991	115.5±13.6	0.217±0.067	1.664
46.50	62.915	131.3± 4.3	0.365±0.035	1.493
49.00	66.099	132.5± 4.0	0.522±0.086	1.426
51.50	69.252	144.0± 2.4	0.519±0.053	4.391
54.00	72.372	127.5± 4.1	0.460±0.077	2.703
56.50	75.458	141.7± 2.2	0.535±0.038	3.511
59.00	78.508	139.2± 2.2	0.811±0.096	2.597
61.50	81.522	153.5± 3.7	0.446±0.047	2.894
64.00	84.497	162.0± 4.6	0.503±0.081	1.456
66.50	87.433	164.9± 6.0	0.389±0.074	1.711
69.00	90.328	144.3± 7.7	0.424±0.120	1.528
74.00	95.993	136.8± 3.3	0.401±0.048	3.226
79.00	101.484	134.8± 3.0	0.295±0.017	1.393
84.00	106.796	154.8± 6.2	0.164±0.017	0.950
86.50	109.384	199.9± 8.0	0.148±0.019	1.182
89.00	111.925	237.0± 4.3	0.245±0.023	1.170
94.00	116.870	237.9± 3.7	0.350±0.037	1.532
96.50	119.273	224.8±12.3	0.363±0.180	0.264
99.00	121.631	189.9± 2.9	0.462±0.044	1.890
101.50	123.943	185.1± 3.3	0.434±0.035	2.797
104.00	126.211	160.7± 5.0	0.330±0.032	0.429
106.00	127.993	147.1± 7.2	0.250±0.035	0.635
106.50	128.434	173.1± 4.3	0.338±0.031	0.705
107.00	128.874	167.6± 8.6	0.197±0.030	1.006
109.00	130.615	144.7±15.4	0.066±0.028	0.940
111.00	132.328	320.1±25.1	0.076±0.042	0.761
111.50	132.752	332.2±13.4	0.084±0.023	1.395
113.00	134.015	310.6±12.8	0.131±0.041	1.324
114.00	134.849	317.3± 5.9	0.188±0.025	1.937
116.50	136.905	306.3± 3.7	0.374±0.049	4.729
119.00	138.922	299.5± 2.7	0.416±0.044	6.447
121.50	140.901	296.6± 5.0	0.432±0.091	3.633
124.00	142.843	285.0± 2.2	0.628±0.116	4.966
126.50	144.750	287.1± 3.6	0.464±0.087	1.867
129.00	146.624	274.4± 2.5	0.596±0.091	3.316
131.50	148.465	264.1± 2.8	0.657±0.229	3.722
134.00	150.275	248.0± 3.5	0.489±0.091	2.283
144.00	157.238	200.8± 3.2	0.464±0.045	1.832
154.00	163.833	141.9± 7.1	0.168±0.021	0.334
159.00	167.026	63.9± 8.9	0.144±0.028	1.625
164.00	170.165	30.5± 8.8	0.391±0.232	2.245

but demonstrates clearly how the pattern becomes essentially isotropic in the reaction plane at scattering angles near certain minima in the inelastic differential cross section. This measurement was repeated five times over a period of five days of running time and similar patterns resulted each time. The patterns at the top and bottom of fig. 7 were recorded at inelastic scattering angles near maxima in the inelastic cross section and each required less than one hour of total running time for the entire measurement. Typical measurement times varied from one hour to one day, depending on the cross section and the distribution of the radiation. The magnesium target provided similar

TABLE 2

$Mg^{24}(\alpha, \alpha'\gamma)$ angular correlation results

$\phi_{\alpha'}$(lab) (degrees)	$\phi_{\alpha'}$(c.m.) (degrees)	δ_2 degrees	a_2	Lexis coeff.
17.70	20.713	67.8± 4.7	0.175±0.019	4.717
19.80	23.158	60.1± 6.0	0.241±0.037	2.806
22.00	25.714	44.3± 5.5	0.364±0.072	0.635
24.15	28.207	30.4± 9.6	0.361±0.139	0.626
26.40	30.809	98.7±37.6	0.070±0.060	2.680
28.70	33.463	79.9± 6.5	0.335±0.058	1.361
31.00	36.110	82.6± 3.1	0.727±0.217	1.280
33.25	38.690	76.3± 3.5	0.567±0.158	0.697
35.60	41.377	75.8± 3.7	0.501±0.103	1.282
38.00	44.111	53.7± 4.6	0.550±0.283	1.935
40.35	46.778	1.3± 5.2	1.000±0.238	15.160
42.75	49.491	255.0±13.1	0.218±0.070	0.622
45.15	52.191	211.1±20.9	0.210±0.092	2.032
45.55	52.640	129.7± 5.7	0.389±0.066	4.256
50.00	57.612	109.4± 6.1	0.518±0.155	3.256
52.60	60.495	95.2± 6.5	0.513±0.303	1.131
55.25	63.418	44.8±10.1	0.350±0.147	1.435
58.10	66.541	19.4±15.4	0.206±0.109	1.086
61.10	69.807	309.1±14.2	0.250±0.081	1.133
64.25	73.210	237.8±13.0	0.235±0.080	1.887
67.00	76.159	192.7± 6.0	0.434±0.083	1.866
69.55	78.874	165.1± 8.4	0.564±0.278	3.860
72.10	81.571	105.0± 7.5	0.530±0.299	1.508
74.60	84.196	128.7±14.5	0.248±0.069	2.600
77.10	86.803	72.1±13.5	0.290±0.131	1.071
79.55	89.340	9.5±19.2	0.240±0.157	0.846
82.00	91.859	274.5±16.0	0.267±0.221	0.690
84.20	94.106	256.1±17.6	0.251±0.124	2.380
85.10	95.020	213.2±20.0	0.208±0.082	3.120
86.50	96.438	224.4±12.7	0.342±0.107	1.842
88.40	98.855	172.8±27.8	0.167±0.087	1.380
91.30	101.255	249.7±22.9	0.153±0.089	0.391
94.75	104.673	243.5±48.2	0.085±0.147	3.219
97.25	107.127	215.8±35.9	0.103±0.102	2.495
99.75	109.562	224.6±20.4	0.180±0.082	1.798
102.25	111.978	175.5±29.5	0.148±0.072	0.733
104.75	114.376	126.5±15.5	0.260±0.104	3.397
107.25	116.755	137.3±18.1	0.205±0.088	0.672

results, but due to the much smaller inelastic cross section ($Q = -1.37$ MeV), the rate of data acquisition was slowed considerably. Cyclotron duty-cycle improvements made between the C^{12} and Mg^{24} runs, however, helped alleviate this difficulty in the Mg^{24} measurements.

Tables 1 and 2 provide a tabulation of the nuclear polarization parameters a_2 and δ_2 as functions of $\phi_{\alpha'}$, the centre-of-mass angle of the inelastically scattered alpha

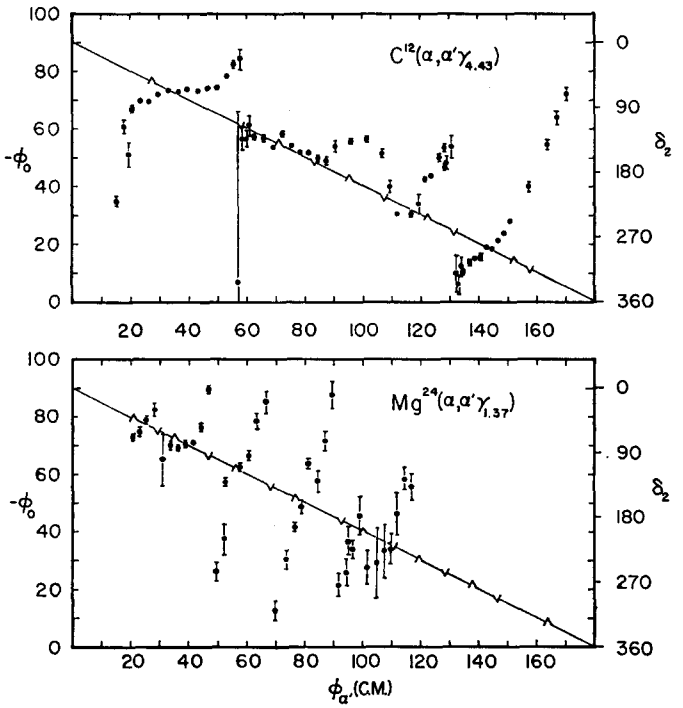

Fig. 8. Plot of the correlation symmetry angle ϕ_0 as a function of centre of mass angle of the inelastically scattered alpha particles, for the reactions $C^{12}(\alpha, \alpha'\gamma)$ and $Mg^{24}(\alpha, \alpha'\gamma)$. Straight lines in both plots indicate the prediction of the adiabatic theory. Carets indicate maxima in the inelastic differential cross section, while inverted carets indicate minima. The polarization phase parameter δ_2 is given on the right scale for comparison.

particle for the reactions $C^{12}(\alpha, \alpha'\gamma_{4.43})$ and $Mg^{24}(\alpha, \alpha'\gamma_{1.37})$, respectively. Where more than one measurement has been made at the same angle, a weighted average of the results has been taken. The errors associated with the determination of the polarization parameters, as discussed above, are given, as are the Lexis coefficients [2]) which characterize the quality of the fit of the correlation function to the data. The empirical parameters A/B and ϕ_0 of equation (1) are not given explicitly in tables 1 and 2, but may be obtained from the simple transformations

$$A/B = (1-a_2)^2/4a_2, \qquad \phi_0 = \tfrac{1}{4}\delta_2. \tag{9}$$

In fig. 8, the correlation symmetry angle ϕ_0 is plotted against $\phi_{\alpha'}$ the centre of mass angle of the inelastically scattered aplha particle, for both the C^{12} and the Mg^{24} angular correlation measurements. The nuclear polarization phase parameter δ_2 is also given for comparison on the right-hand scale. This figure is given for comparison with similar ones in the papers of Blair and Wilets [14]) and of McDaniels *et al.* [5]).

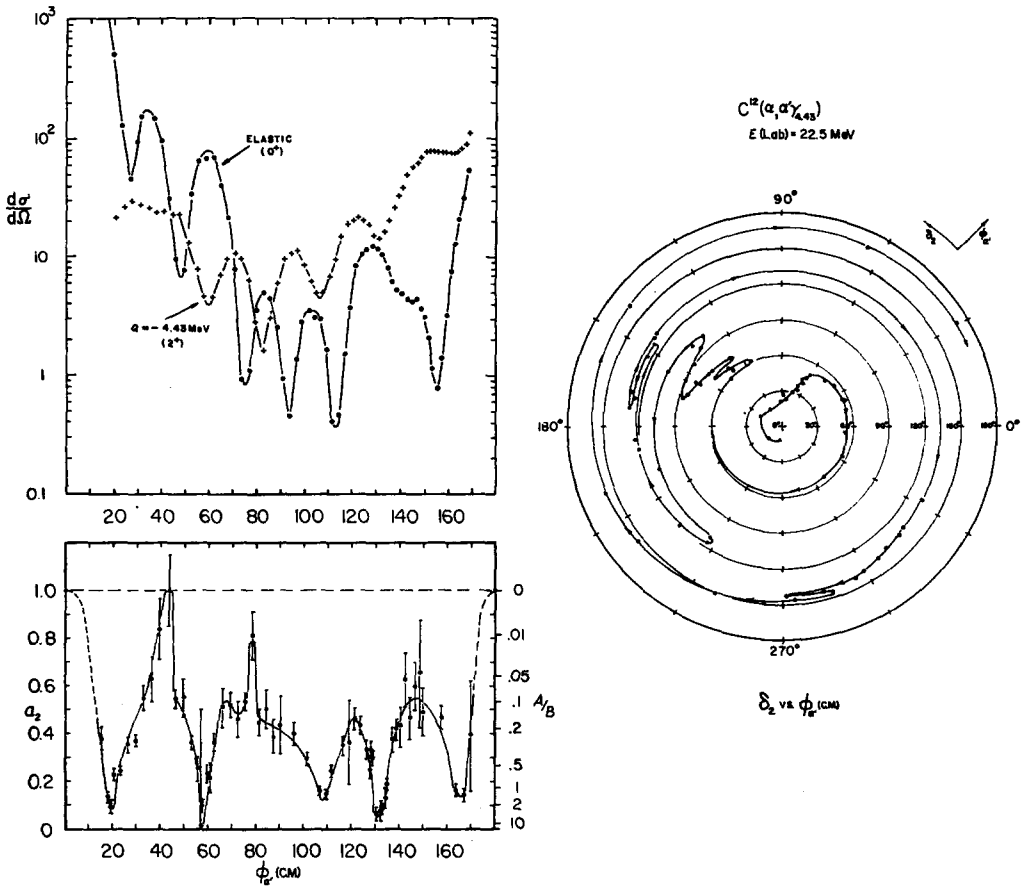

Fig. 9. Polarization parameters a_2 and δ_2 as functions of scattering angle for the reaction $C^{12}(\alpha,\alpha'\gamma)$. Elastic and inelastic differential cross sections are given for comparison. The empirical parameter A/B of eq. (1) is also given on the right side of the a_2 plot for comparison. The polarization phase parameter δ_2 is plotted as the angular coordinate to the polar plot shown while the scattering angle is plotted as the radial coordinate. The polar plot of the phase parameter emphasizes its periodic cyclic behaviour which appears as discontinuities in fig. 8.

The symmetry angle ϕ_0 is periodic in 90° intervals and is plotted here between −90° and 0° so that it may be compared with the angles of elastic and inelastic recoil, both of which are found in this angular interval. For this reason, the negative of the symmetry angle is actually the quantity plotted.

In fig. 8 the directions of elastic recoil are indicated by straight lines and the maxima and minima of the inelastic scattering differential cross section are indicated by upright and inverted carets, respectively, on these lines. The striking feature of this figure is the manner in which the symmetry angles of both correlation measurements undergo rapid sweeps through 90° which invariably correspond to a minimum in the

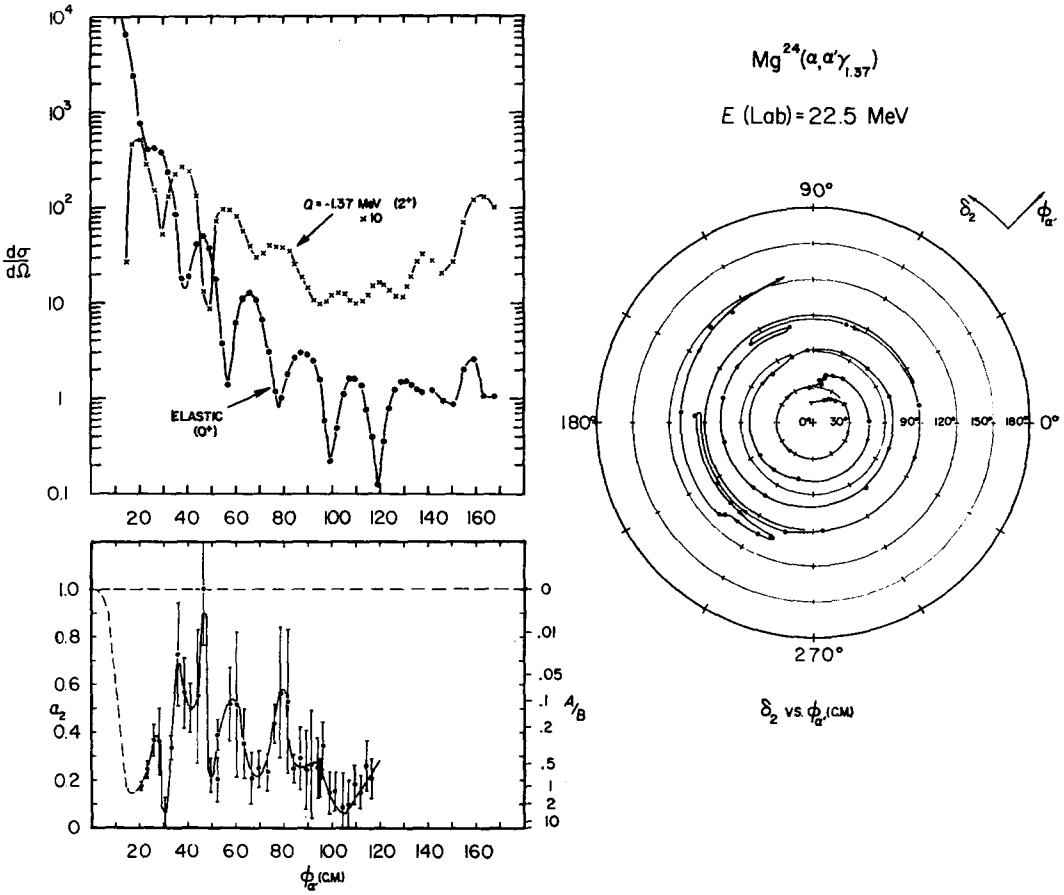

Fig. 10. Polarization parameters a_2 and δ_2 as functions of scattering angle for the reaction Mg^{24} $(\alpha, \alpha'\gamma)$. Elastic and inelastic cross sections and A/B values are given as in fig. 9.

inelastic scattering differential cross section. This behaviour seems to be characteristic of $(\alpha, \alpha'\gamma)$ correlations [2, 5, 15, 24]), but has not been observed in $(p, p'\gamma)$ correlations [4, 6, 16–23]). It should be noted that these 90° shifts occur more regularly in the Mg^{24} data than in the C^{12} data, and that there are minima in the cross sections of both target nuclei which are *not* accompanied by 90° sweeps of the symmetry angle. In the next section this behaviour will be compared with the predictions of applicable theories.

In figs. 9 and 10 the nuclear polarization parameters a_2 and δ_2 are plotted against $\phi_{\alpha'}$, the centre-of-mass angle of the inelastically scattered alpha particle, for C^{12} and Mg^{24}, respectively. The differential cross sections for elastic and inelastic scattering

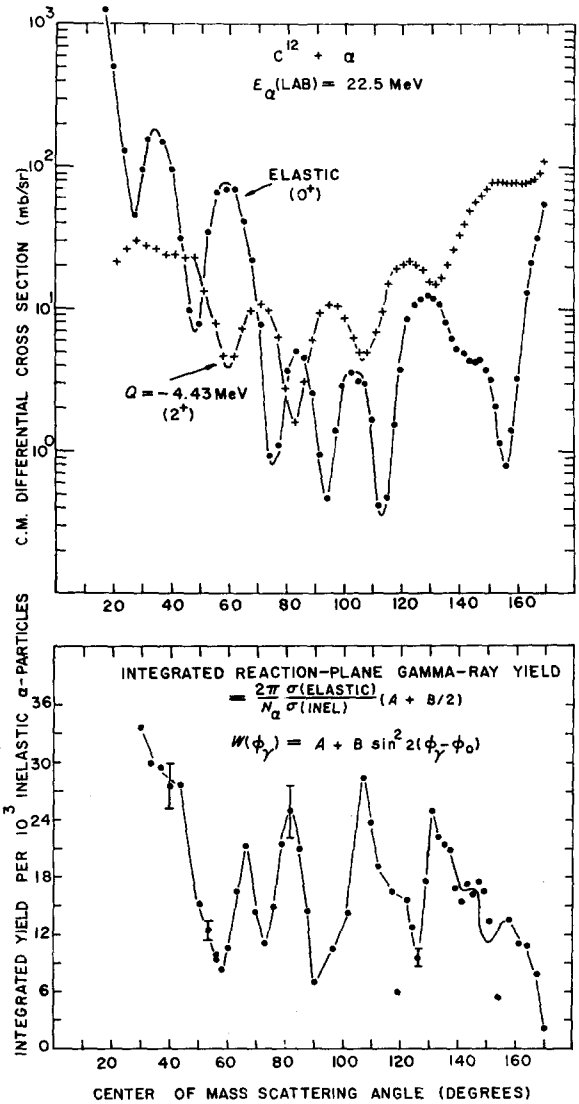

Fig. 11. Experimentally determined reaction plane gamma-ray yield as a function of scattering angle for the reaction $C^{12}(\alpha, \alpha'\gamma)$. Elastic and inelastic differential cross sections are given for comparison.

are also presented in these figures. The polarization phase parameter δ_2 is plotted in these figures in polar coordinates, with δ_2 as the angular coordinate and $\phi_{\alpha'}$ as the radial coordinate. This presentation emphasizes the periodic cyclic behaviour of the

relative phase of the $m = 2$ and -2 substates, as given by δ_2. The phase parameter thus appears as a spiral, and as noted in fig. 8, the phase parameter for Mg^{24} behaves more regularly than that for C^{12}. A recent correlation measurement on Si^{28} shows behaviour similar to that of Mg^{24} in this respect [24]).

The nuclear polarization amplitude parameter a_2, as given in figs. 9 and 10, represents the ratio of amplitudes of the $m = 2$ substate to the $m = -2$ substate. As discussed in the previous paper [1]), there is an ambiguity in the determination of this parameter, unless gamma-ray polarizations are measured, which arises from the fact that $1/a_2$ gives rise to a correlation function which is identical to that of a_2. Thus, while the interval of a_2 in figs. 9 and 10 is restricted to the range of 0 to 1.0, the reciprocal of each value of a_2 is understood to be an equally valid result of the correlation measurements. On the right-hand scale of these figures the values of the empirical correlation parameter A/B, as used in eq. (1), are given. The extrema of scattering angle, 0° and 180°, lie along the beam direction and for these angles both the reaction plane and the z-axis are undefined. Therefore the parameter a_2 must have the value 1, and so two "free" points are known in advance and are shown in these figures.

It is apparent from figs. 9 and 10, that a_2 is not, in general, equal to one, as predicted by the semi-classical, plane wave, and adiabatic theories which will be described below. Rather, this parameter shows regular variations between 0 and 1, and in particular the minima correspond to minima in the differential cross section for the inelastic scattering. Thus the rapid changes of the phase parameter and the minima of the amplitude parameter are correlated, and may be different manifestations of the same effect.

Another type of information may be obtained from these correlation measurements by summing the data to obtain the total gamma-ray yield in the reaction plane. This type of analysis has been performed on the C^{12} data and is shown in fig. 11 as a function of $\phi_{\alpha'}$. Since only gamma rays from the $m = 2$ and -2 substates can be emitted in the reaction plane, the integrated reaction-plane gamma-ray yield gives some indication of the degree to which the $m = 0$ substate is populated (strong population of this state corresponds to a minimum in the reaction plane yield.) The reaction plane yield Y, as given in this figure, has been normalized to remove any dependence on the differential cross section by dividing out this dependence. The most distinctive feature of this figure is the correspondence between the forward maximum of the inelastic differential cross section and general rise of the gamma-ray yield at forward angles, as contrasted with the drop in gamma-ray yield at backward angles where there is also a maximum in the cross section. The correspondence between the first minimum in the cross section and in the gamma-ray yield should also be noted, and will be discussed below.

4. Discussion of Theory

The angular correlation measurements of the $C^{12}(\alpha, \alpha'\gamma)$ and $Mg^{24}(\alpha, \alpha'\gamma)$ reactions, which were presented in the preceding section, show many interesting and distinctive

features. If these measurements are to become more than just experimental curiosities, however, it is necessary to relate them, at least qualitatively, to the theoretical calculations which are relevant in this area. The form of analysis of the data makes this particularly straightforward, because the experimental results may be compared directly with the scattering amplitudes predicted by the various theories.

Since, in the present experiments, no angular correlations were measured out of the reaction plane, the determination of the nuclear polarization is incomplete, in that the a_0 and δ_0 polarization parameters have not been measured. Therefore, the scattering amplitudes cannot be reconstructed completely, and the comparison must go the other way, comparing the derived relative phases and magnitudes of the scattering amplitudes with the parameters a_2 and δ_2. Work now in progress will allow extraction of all four polarization parameters and full reconstruction of the scattering amplitudes.

4.1. SEMI-CLASSICAL APPROXIMATION

The simplest theoretical approach to the problem of predicting nuclear polarizations and angular correlations comes from the semi-classical model [25]). In this model, the interaction is presumed to occur at a specific point in the nuclear volume denoted by the coordinate $\boldsymbol{r}$. The transferred momentum $\boldsymbol{L}$ in the reaction is therefore associated with the transferred linear momentum $\boldsymbol{p}$ by the relation $\boldsymbol{L} = \boldsymbol{r} \times \boldsymbol{p}$. This tells us immediatley that $\boldsymbol{L}$ and $\boldsymbol{p}$ are perpendicular, so the angular momentum has no projection along the direction of transferred momentum, i.e., the direction of the recoiling nucleus. For alpha particles scattered from an even nucleus, this means that with the quantization axis taken along the recoil direction, only the $m = 0$ angular momentum substate will be populated in the reaction. Therefore the set of scattering amplitudes T_{jm} will be given by $T_{jm} = \overline{T_j}\,\delta_{m0}$. Rotation of the coordinate system to one in which the x-axis is in the beam direction and the z-axis is perpendicular to the reaction plane [1]) gives, for the case where the angular momentum of the excited nucleus is $j = 2$, the relations

$$T_{2\pm2} = \sqrt{\tfrac{3}{8}}\,T_2 e^{\pm 2i\phi_r}, \qquad T_{2\pm1} = 0, \qquad T_{20} = -\tfrac{1}{2}\overline{T_2}, \tag{10}$$

where T_2 is the overall amplitude and ϕ_r is the direction of the recoiling excited nucleus, measured in a *positive* sense from the x-axis. The polarization parameters given by these amplitudes are

$$\begin{aligned} a_2 &= 1, & \delta_2 &= 4\phi_r, \\ a_0 &= \sqrt{\tfrac{2}{3}}, & \delta_0 &= 2\phi_r + \pi. \end{aligned} \tag{11}$$

In the reaction plane, the correlation function predicted from these parameters is a well behaved sinusoid of the form $W_2(\frac{1}{2}\pi, \phi) \propto \sin^2 2(\phi - \phi_r)$. Thus the A coefficient of eq. (1) vanishes and the symmetry angle ϕ_0 is just the recoil angle ϕ_r. These predictions, however, bear little similarity to the measurements presented above in figs. 8-10.

Moreover, the total gamma ray yield in the reaction plane can be calculated from the amplitudes. Since only the $m = \pm 2$ substates give rise to radiation in the reaction plane for the $j = 2$ case, the integrated yield of gamma rays arising from these substates will be proportional to the reaction plane yield:

$$Y(\theta_{\alpha'}) \propto [|T_{22}|^2 + |T_{2-2}|^2] / \sum_m |T_{2m}|^2 = \tfrac{1}{4}T_2^2 / \overline{T_2^2} = \tfrac{1}{4}. \tag{12}$$

Thus the prediction of the classical approximation is that the yield of reaction plane gamma rays, the experimental values of which are given in fig. 11, should be constant with scattering angle. Clearly, this prediction is somewhat at variance with the experimental results given in fig. 11.

4.2. THE PLANE-WAVE BORN APPROXIMATION

A somewhat more realistic prediction of the amplitudes might be expected from a plane-wave Born-approximation (PWBA) calculation, since a quantum mechanical calculation should more closely represent the true situation than the semi-classical approach. However, this type of calculation has been carried out by Satchler [26, 27]) and the results for α-particle scattering are exactly the same as those given by the semi-classical model, as stated above, and are, therefore, also in disagreement with the experimental results presented in this paper.

4.3. ADIABATIC APPROXIMATION

Another approximate theory which has been used to predict alpha-gamma correlation functions and gives the results in a simple closed form is the adiabatic approximation [28, 29]). Such a calculation was used by Blair and Willets [14]) to predict the correlation function for a $j = 2$ excited state. However, since this calculation was limited to the reaction plane, they were able to obtain this function without actually calculating the scattering amplitudes by the use of symmetry relationships [30]). It is possible to obtain these amplitudes, however, by using the methods employed in the earlier paper of Blair [29]), with the modification that the shadow plane of that calculation is made to follow the recoil axis instead of remaining perpendicular to the beam axis. Appendix 1 of this paper shows this calculation. The amplitudes which are predicted are

$$\begin{aligned} T_{2\pm 2} &= -C\sqrt{\tfrac{3}{2}}(J_2(x) - J_0(x))e^{\pm 2i\phi_R}, \qquad T_{2\pm 1} = 0, \\ T_{20} &= C(3J_2(x) + J_0(x)), \end{aligned} \tag{13}$$

where $C = ikR_0^2\beta/8\pi^{\frac{1}{2}}$, β is the nuclear deformation parameter; $x = 2kR_0 \sin\frac{1}{2}\phi$, is the argument of the Bessel functions, k is the incident particle wave number, R_0 is the nuclear radius, and ϕ_R is the direction of *adiabatic* recoil, i.e., the recoil direction for elastic scattering.

The polarization parameters given by these amplitudes are

$$\begin{aligned} a_2 &= 1, & \delta_2 &= 4\phi_R, \\ a_0 &= \sqrt{\tfrac{2}{3}}\left|\frac{3J_2 + J_0}{J_2 - J_0}\right|, & \delta_0 &= 2\phi_R + \pi (= 2\phi_R \text{ at zero gaps}) \end{aligned} \tag{14}$$

The Bessel functions here all have the argument x defined above; the phase parameter δ_0 will change discontinuously by π over small regions of x where the numerator and denominator in the a_0 expression are different in sign, referred to above as zero gaps (see appendix 1).

As in the classical and PWBA predictions described above, the correlation function in the reaction plane is of the form $W(\frac{1}{2}\pi, \phi) \propto \sin^2 2(\phi - \phi_R)$, but here the symmetry axis follows the *adiabatic* recoil direction. This is the result obtained by Blair and Willets [14]), and they have shown that it compares favourably with a number of measurements of (p, p'γ) angular correlations [4, 16–19]) and is consistent with the (α, $\alpha'\gamma$) correlation measurements of Schook [15]), taken at a few scattering angles with 43 MeV alphas on C^{12} and Mg^{24}.

The predictions of the adiabatic theory for $j = 2$ angular correlations in the reaction plane differ from the semi-classical and PWBA predictions in only one rather minor detail: the symmetry axis of the correlation function is along the *adiabatic* recoil direction rather than along the *actual* recoil direction. This difference is difficult to observe except in very light nuclei at extreme forward angles. Moreover, it is not completely clear whether this difference should properly be taken as a criterion for judging the relative merits of the theories, since this difference in recoil directions may well be an artifact of the adiabatic assumption itself. In the PWBA and semi-classical calculations, the questionable assumption can be made that the initial and final particle momenta are equal in magnitude. These theories then give the *same* prediction in the reaction phase as the adiabatic theory. It is difficult, however, to see how the validity of these calculations is improved by this assumption. In any case, none of the three theories described above is particularly successful in predicting the behaviour of the observed reaction plane correlations.

There are, however, essential differences between the adiabatic theory and the other two mentioned which should make it possible to distinguish between them when any of them have any validity. While predictions of the theories for the polarization parameters a_2 and δ_2 are virtually identical, the paramaters a_0 and δ_0 are quite different in the adiabatic theory than in the other two. In particular the phase parameter δ_0, while corresponding to the PWBA prediction at most angles, has discontinuities of π at the zero gaps described in the appendix. Moreover, the parameter a_0 is predicted by adiabatic theory to have strong angular dependence, while S-C and PWBA theories predict that it has a constant value of $\sqrt{\frac{2}{3}}$. These predictions should be easily observable in correlations measured out of the reaction plane.

In addition, adiabatic theory predicts angular dependence for the integrated reaction-plane gamma-ray yield, in contrast to the constant behaviour predicted by the S-C and PWBA theories. As shown before, this reaction-plane yield $Y(\theta_{\alpha'})$ is proportional to the $m = \pm 2$ substate yield, so that

$$Y(\theta_{\alpha'}) \propto [|T_{22}|^2 + |T_{2-2}|^2] / \sum_m |T_{2m}|^2 = \tfrac{3}{4} \frac{(J_2 - J_0)^2}{3J_2^2 + J_0^2} . \qquad (15)$$

This function is illustrated in fig. 12. It rises periodically to a value of 1, and then drops steeply to zero and begins another rise. In particular, minima of this function correspond closely (though not exactly) to minima of the inelastic cross section as predicted from the adiabatic approximation. The latter is also given in fig. 12 for comparison. Examination of fig. 11 shows that there are approximately coincident minima in the inelastic cross section and the reaction-plane gamma-ray yield near $\phi_{\alpha'} = 60°$. There is no correspondence, however, between the minima which occur at larger angles, and the general shape of the experimental reaction-plane yield bears

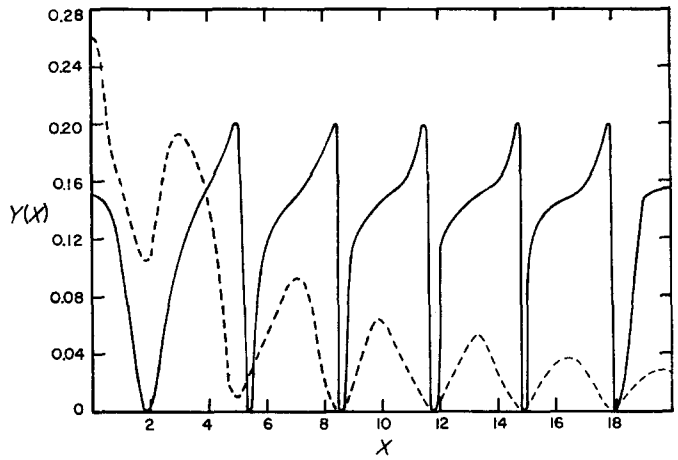

Fig. 12. Reaction plane gamma-ray yield as predicted by adiabatic theory is given by solid line. Dashed curve is adiabatic prediction for inelastic scattering differential cross section. Note the correspondence of the minima.

little resemblance to the calculated function. The adiabatic approximation is expected to have greater validity at small angles, and the correspondence of the forward minima is consistent with this idea.

4.4. DISTORTED-WAVE BORN APPROXIMATION

The theories discussed above make it possible, by virtue of their simplifying assumptions, to write the predicted scattering amplitudes in a simple closed form. Distorted-wave Born-approximation (DWBA) calculations give predictions for the scattering amplitudes which cannot be written in closed form, and require detailed numerical evaluation to obtain predictions for a specific nuclear reaction. This prevents a direct comparison of DWBA predictions with the predictions of the simpler theories.

Distorted-wave Born-approximation calculations of nuclear polarization and angular correlations have been made at this laboratory. Calculations of this type put stringent conditions on the choice of optical model parameters, since the calculation must correctly predict the elastic and inelastic differential cross section as well as the angular correlations. The results of these calculations are not completely satisfactory

as yet and will be reserved for discussion in a latter paper [31]). However, it is possible to make some general remarks about the predictions obtained from DWBA calculations, based on the calculations mentioned above and those of Bassel and Satchler [5, 32]).

(i) The amplitudes T_{22} and T_{2-2} are not usually equal, so that a_2 usually differs from 1 and the correlation function has a definite isotropic component. This prediction is in contradiction to the predictions of all three of the simple theories discussed above, all of which predict that $T_{22} = T_{2-2}$, $a_2 = 1$, and the correlation function has no isotropic component but goes to zero at the minima. The DWBA predictions for a_2 and a_0 vary regularly between 0 and 1 and are in qualitative agreement with experimental results, as given in figs. 9–11 and in ref. [5]).

(ii) The DWBA prediction for the phase parameter δ_2 is strongly dependent on the choice of optical model parameters used in the calculation, and one such prediction [27, 33]) may closely approximate (p, p'γ) experimental results [4, 6, 17–23]) and the predictions of the simple theories discussed above, while another may predict rapid shifts in δ_2 of the type present in the (α, $\alpha'\gamma$) experimental results presented above. Roughly speaking, the predictions which correspond to those of the simple theories are obtained in calculations involving small level excitation energies, low absorption potentials, high scattering potentials and high bombarding energies, while predictions of rapid variations of δ_2 generally correspond to large level excitation energies, high absorption potentials, and scattering potentials and bombarding energies in the medium range. It is also found that sets of optical parameters which give similar predictions for differential cross sections [34]) may give radically different predictions for the angular correlations and nuclear polarization parameters.

Thus the DWBA calculations can qualitatively predict the observed behaviour of angular correlations and nuclear polarization, and in at least one case, reasonably good fits to such data at forward angles have been obtained [5]). Unfortunately, such calculations fail to provide any simple physical explanation of the striking behaviour of the polarization parameters, particularly the phase parameter δ_2. So distinctive a phenomenon should have a simple physical explanation, and work now in progress at this laboratory shows promise of providing such an explanation [31]).

4.5. COMPOUND NUCLEUS FORMATION

It is tempting to take the partial success of the DWBA calculations in predicting the distinctive phase behaviour of the observed (α, $\alpha'\gamma$) correlations as evidence for the dominance of a direct reaction mechanism in this reaction. The validity of such a generalization remains in question, however, until the predictions of compound nucleus theory bearing on this experiment are calculated and until the expected interference between the compound and direct processes is well understood. Such an investigation implicitly involves the calculation of a set of scattering amplitudes predicted for the reaction from compound nucleus theory, and this general calculation without simplifying assumptions remains one of the outstanding problems of nuclear theory.

This calculation can, however, be carried out in the two extreme cases, one assuming that only one isolated level is excited in the compound nucleus and the other assuming that very many overlapping levels in the compound nucleus are excited and the statistical assumption can be made [38, 39]). The single-level approach seems rather unrealistic for the reactions studied here, since the compound nuclei formed in both cases would have excitations in excess of 25 MeV and the density of states would be quite high. Nevertheless, the predictions of this calculation are of interest as a limiting case.

The single-level calculation of the angular correlation function makes use of the single-level formula [35, 37]), along with the angular momentum formalism appropriate to this calculation [36, 37]). If the state excited in the compound nucleus has spin J, and the compound nucleus decays to a 2^+ state, then the angular momentum of the outgoing alpha particle can have only the values $J+2$, J and $J-2$ and these transitions can have coherent interference which complicates the problem. However, it is expected that the effect of the angular momentum barrier [35]) will be to strongly select the lowest angular momentum, i.e., $J-2$, and the calculation is greatly simplified by making this assumption.

The details of this calculation depend on the value of J and will not be presented here, but the general results of such calculations can be summarized as follows.

(i) The single-level calculation can predict rapid sweeps in the symmetry angle and phase parameter similar to those present in the experimental results presented above. However, this behaviour requires that the resonance have a fairly high angular momentum, and the results presented above would imply that $J \cong 8$ for C^{12} and $J \cong 10$ for Mg^{24}.

(ii) Interference from neighbouring levels or from competing transitions of higher angular momentum in the same level are likely to wash out the rapid changes in the symmetry angle described above.

(iii) The $m = 2$ and -2 angular momentum substates in the final nucleus will be equally populated, independent of the angle, at which the alpha particle is inelastically scattered. Thus the polarization parameter a_2 will always have the value 1 and the correlation function will go to zero at its minima for all alpha particle scattering angles. This prediction is inconsistent with the small values of a_2 and the large isotropic components of the correlation function which were observed experimentally at some scattering angles.

The other limiting case which can be calculated used the assumption that there are a large number of states populated in the compound nucleus, and that due to the overlapping of these states and the finite energy spread of the beam (about 150 keV in the experiment described above) the interference between states is completely averaged out. This is the approach of the Hauser-Feshbach theory [38, 39]). Using this formalism, the differential cross sections and correlation functions of interest can be calculated from transmission coefficients [35]) derived from the optical model. The assumptions of this type of calculation seem more realistic than those of the single-level approach,

particularly in measurements such as those presented above, in which the large spread in beam energy would be expected to strongly average the fast variations in phase associated with compound nucleus phenomena and to greatly attenuate interference effects.

Calculations of this type have been applied to (p, p'γ) angular correlation measurements by Seward [16]) and Sheldon [40,41]) for protons at low bombarding energies where there is virtually no contribution to the reaction from incoming and outgoing partial waves having angular momentum greater than 2. The restriction to angular momentum values less than or equal to 2 is, of course, completely invalid for the scattering of 22.5 MeV alpha particles, and so the results of these calculations cannot be directly applied. Moreover, calculation of the correlation function for the alpha particle case requires a rather complicated numerical calculation.

Fortunately, a good deal of information about the correlation function may be obtained by examination of its formal expression [42]).

(i) At bombarding energies just above the reaction threshold the outgoing alpha particles must have zero angular momentum, and both the Hauser-Feshbach theory and the direct reaction theory predict that the reaction plane correlation function will have the form $W(\phi) = \sin^2 2\phi$. This function is independent of the scattering angle $\phi_{\alpha'}$ and is symmetric about the beam direction and about 90°.

(ii) As more angular momentum values are included in the Hauser-Feshbach calculation (as energy is increased) the correlation function symmetry angle ϕ_0 will begin to deviate from 90° and show variations with scattering angle, but it appears unlikely that variations as pronounced as those present in the experimental results given above can be predicted.

(iii) As more angular momentum values are included, the correlation function will become more isotropic, i.e., the maxima and minima of the correlation function will be averaged over and the function will become more uniform. It appears unlikely that the deep minima experimentally observed in the correlation function at some scattering angles (corresponding to values of a_2 near 1) can be predicted by this theory.

(iv) If poor energy resolution and fast variations of scattering amplitude phase with energy are actually present in an experimental determination, as implied by the statistical assumption of the Hauser-Fesbach theory, then it is not meaningful to analyse the observed correlation function in terms of nuclear polarization as described above [1]), since the correlation function is actually a superposition of many dissimilar correlation functions produced by the different energy components of the beam. On the other hand, the part of the reaction produced by the compound nucleus reaction mechanism under these circumstances would not be expected to interfere with the direct reaction contribution and could be calculated and subtracted as background from the experimental correlation function before the analysis for nuclear polarization was performed. This does not seem to be necessary in the present experimental results on the basis of the observation of a_2 values near 1 at some scattering angles, which apparently rules out a sizable compound-nucleus contribution of the Hauser-Feshbach type in the reaction process.

Thus neither of the extremes of compound nucleus theory seems able to explain the observed behaviour of a_2, the single-level approximation predicting that a_2 is always 1 while the Hauser-Feshbach theory seems to predict that a_2 is always small. Experimental results, on the other hand show strong variations of a_2 between 0 and 1, so that neither of these predictions is valid at all angles, although both are correct at some. Further calculations in this area are needed to determine whether some intermediate case of compound nucleus theory can obtain the agreement with experimental elastic and inelastic scattering cross sections and angular correlations presently obtainable with DWBA calculations.

5. Conclusion

In the above discussion, it has been shown that analysis of the angular correlation data for the $C^{12}(\alpha, \alpha'\gamma_{4.43})$ and the $Mg^{24}(\alpha, \alpha'\gamma_{1.37})$ reactions in terms of the nuclear polarization parameters has provided a strong basis for comparing the experimental results with the predictions of the simpler theories and discussion of the more complex theories. This was possible because analysis in terms of polarization highlights the essential information contained in angular correlation measurements. It also brings out the important point that correlation measurements which are restricted to the reaction plane, as was the case in the present experiment, represent an incomplete determination, in that half of the unknown nuclear polarization parameters (a_0 and δ_0) have not been determined. To complete such a determination it is necessary to measure the angular correlations also out of the reaction plane. With this measurement and the differential cross section it is then possible to completely reconstruct the set of scattering amplitudes T_{jm}, within an overall phase. Such measurements are now in progress.

It was seen that the analysed experimental results of this and other [5, 24]) $(\alpha, \alpha'\gamma)$ angular correlations showed striking and distinctive behaviour which had not been observed in $(p, p'\gamma)$ angular correlation measurements [4, 6, 16–23]). This behaviour seems to be characterized by strong maxima and minima as a function of scattering angle in the parameter a_2, which reflects the relative intensities of the $m = 2$ and -2 substates, and by rapid variations of the phase parameter δ_2 through repeated 360° cycles as a function of scattering angle. Further, the reaction plane yield of gamma radiation was found to also undergo strong fluctuations with scattering angle.

In the subsequent discussion of theories bearing on angular correlations, it was shown that there is little agreement between these experimental results and the simple direct reaction theories which include the semi-classical model [25]), the plane-wave Born-approximation [26]), and the adiabatic diffraction model [29]), although there may be some areas of agreement with the latter at the forward angles. On the other hand, the more computationally difficult distorted-wave Born-approximation theory [33]) seems to give predictions which are at least qualitatively in agreement with the experimental results, particularly in the behaviour of the phase parameter δ_2 [5, 24, 31]).

Single-level compound-nucleus theory [35]) seems able to roughly predict the observed correlation phase behaviour only when rather unrealistic assumption are made. Compound nucleus calculations of the Hauser-Feshbach type, [38,39,42]) which assume the averaging of many levels in the compound nucleus, predict a high degree of isotropy in the correlation functions, and are thus inconsistent with experimental results at many angles.

Thus the comparison of the experimental results of angular correlation measurements with theoretical predictions has provided a strong basis for the criticism of the various theoretical approaches, for differential cross sections and angular correlation measurements are only slightly different ways of viewing the same reaction process, and a theory which correctly predicts the first without predicting the second is no better than a theory which predicts the differential cross section at some angles but not at others.

Perhaps more important, recent progress has been made toward development of a unified theory of nuclear reactions [43]) which implicitly includes direct reactions, compound nucleus formation, and interference between the two [44]). It appears that an excellent way of investigating such interference effects would be through angular correlation measurements of the type presented above, but performed over a range of energies with thin targets and very good beam energy resolution so that coherent interference effects would not be averaged out. Since coherent interference between reaction mechanisms is determined by the phase difference in the amplitudes of the two processes, it might be expected to have a pronounced effect on the phase parameters determined from angular correlation measurements made in this way. Therefore correlation measurements of the type presented in this paper can be expected to play an increasingly important role in the study of reaction mechanisms.

We are indebted to Dr. John G. Wills for helpful suggestions on theoretical analysis and for critical reading of the manuscript. We also appreciate constructive comments by Professor Marc Ross and Dr. G. R. Satchler concerning the interpretation of our results.

Appendix

ADIABATIC DIFFRACTION MODEL CALCULATION OF SCATTERING AMPLITUDES

The original paper of Blair [29]) on diffraction scattering in the adiabatic approximation predicts implicitly that the symmetry axis of the correlation function will always lie along the beam axis. This incorrect result arises from the fact that the shadow plane, i.e., the plane through the centre of the nucleus on which the nucleus is projected as a disc for the purposes of the diffraction calculation, is assumed to be perpendicular to the beam. Clearly, this assumption will be invalid beyond 90° and can reasonably be expected to work only at small angles.

As Blair suggested later in the paper, [29]) a better choice for the shadow plane seems to be the plane which includes the direction of motion of the recoiling excited nucleus,

which in the adiabatic approximation is the negative of the bisector of the centre-of-mass scattering angle. The x-axis is now chosen as the anti-recoil direction in the shadow plane, and the z-axis is chosen perpendicular to the shadow plane and lies along the beam direction when the scattering angle Θ is zero. Both the x and z axes lie in the reaction plane. This coordinate system is illustrated in fig. 12.

The Fraunhofer approximation for the amplitude of scattering from this shadow plane then becomes

$$f(\alpha) = (ik_i/2\pi)\iint e^{-i(k_i - k_f)\cdot r} dA. \tag{16}$$

When this is used in place of Blair's equation (21), and k_i is set equal to k_f under the adiabatic approximation, the amplitude is given to first order in α by

$$f(\alpha, \Theta) = (ik/2\pi)\int_0^{2\pi} d\varphi \left[\int_0^{R_0} e^{-2ikr \sin \frac{1}{2}\Theta \cos \varphi} r\, dr + e^{-2ikR_0 \sin \frac{1}{2}\Theta \cos \varphi} R_0^2 \sum_{jm} \alpha_{jm} Y_j^m(\tfrac{1}{2}\pi, \varphi)\right]. \tag{17}$$

This expression is identical to that of Blair except for the substitution of the argument $2\sin\frac{1}{2}\Theta$ for Θ, and the integrals will thus differ only in this argument. Thus the amplitude after integration is

$$f(\alpha, \Theta) = ikR_0^2 \left[\frac{J_1(2kR_0 \sin \frac{1}{2}\Theta)}{2kR_0 \sin \frac{1}{2}\Theta} + \sum_{j+m \text{ even}} i^j J_m(2kR_0 \sin \tfrac{1}{2}\Theta) \left(\frac{2j+1}{4\pi}\right)^{\frac{1}{2}} \frac{((j-m)!(j+m)!)^{\frac{1}{2}}}{(j-m)!!(j+m)!!} \alpha_{jm}\right]. \tag{18}$$

The scattering amplitudes for exciting a state of spin j and spin projection m in an even nucleus by inelastic scattering are

$$T_{jm}(\Theta) = \langle jm | f(\alpha, \Theta) | 0\,0 \rangle. \tag{19}$$

For the case of interest here, $j = 2$ and $m = 0, \pm 1$, and ± 2. Since the sum in the above expression contains only terms for which j-m is even, the amplitudes $T_{2\pm 1}$ have value zero. The other amplitudes have the form

$$\begin{aligned} T_{22}(\Theta) &= -ikR_0^2 \langle 22|\alpha_{22}|00\rangle (5/4\pi)^{\frac{1}{2}} \sqrt{\tfrac{3}{8}}\, J_2(2kR_0 \sin\tfrac{1}{2}\Theta), \\ T_{20}(\Theta) &= -ikR_0^2 \langle 20|\alpha_{20}|00\rangle (5/4\pi)^{\frac{1}{2}} \tfrac{1}{2} J_0(2kR_0 \sin\tfrac{1}{2}\Theta), \\ T_{2-2}(\Theta) &= -ikR_0^2 \langle 2-2|\alpha_{2\,-2}|00\rangle (5/4\pi)^{\frac{1}{2}} \sqrt{\tfrac{3}{8}}\, J_2(2kR_0 \sin\tfrac{1}{2}\Theta). \end{aligned} \tag{20}$$

To evaluate the expectation values of the alpha coefficients, we may apply the Wigner-Eckhart theorem [45]):

$$\langle jm|\alpha_{jm}|00\rangle = C(0jj;\, 0mm)\, \langle j||\alpha_j||0\rangle = \langle j||\alpha_j||0\rangle. \tag{21}$$

Further, the α's are the expansion coefficients of the nuclear radius in spherical harmonics. This radius is real, so the coefficient α_{j0} must be real, leading to the conclusion

from the equalities above that $\langle j||\alpha_j||0\rangle$ is a real number. Blair [29]) gives the value of its absolute square as $\hbar\omega_j/2C_j$. This may be rewritten in terms of of the nuclear deformation parameter β_j as ${\beta_j}^2/(2j+1)$. Thus the scattering amplitudes have the values

$$\begin{aligned} T_{2\pm2} &= -ikR_0^2\beta(4\pi)^{-\frac{1}{2}}\sqrt{\tfrac{3}{8}}\,J_2(2kR_0\sin\tfrac{1}{2}\Theta), \\ T_{20} &= -ikR_0^2\beta(4\pi)^{-\frac{1}{2}}\tfrac{1}{2}\,J_0(2kR_0\sin\tfrac{1}{2}\Theta). \end{aligned} \tag{22}$$

Thus far, this calculation has been carried out in a rather curious coordinate system in which the quantization axis changes as a function of scattering angle and is always perpendicular to the recoil direction and in the reaction plane. We now wish to transform the amplitudes into those appropriate to the coordinate system where the beam is the x-axis and the z-axis is perpendicular to the reaction plane in the $\boldsymbol{k}_i \times \boldsymbol{k}_f$ direction. These coordinate systems are shown in fig. 13.

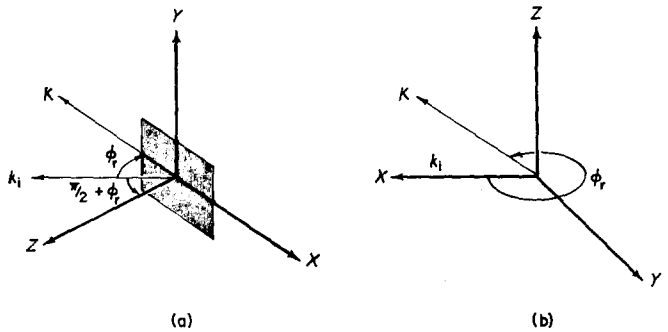

Fig. 13. Coordinate systems used in (a) adiabatic calculation and (b) discussion of polarization parameters. The beam direction is indicated as k_i, the direction of momentum transfer (recoil direction) as K, and the angle between k_i and K is labelled ϕ_r. The shadow plane used in the adiabatic calculation is indicated by the shaded rectangle in (a).

This rotation is accomplished by means of the rotation operator [1,45])

$$D^j_{m'm}(-\tfrac{1}{2}\pi, -\tfrac{1}{2}\pi, -(\tfrac{1}{2}\pi+\phi_R)) = i^{m'+m}d^j_{m'm}(-\tfrac{1}{2}\pi)e^{im\phi_R}, \tag{23}$$

and the reduced rotation operator $d^j_{m'm}(-\frac{1}{2}\pi)$ has the values

$$d^2_{2\pm2} = \tfrac{1}{4}, \qquad d^2_{0\pm2} = d^2_{\pm20} = \sqrt{\tfrac{3}{8}}, \qquad d^2_{00} = -\tfrac{1}{2}. \tag{24}$$

These are the only values of this operator which are actually needed to perform the desired rotation, since the $m' = \pm 1$ amplitudes are zero in the old coordinate system, and we know from the Bohr theorem [1,46]) that the $m = \pm 1$ amplitudes in the new system will also be zero.

Performing this rotation and writing the arguments of the Bessel functions as $x = 2kR_0\sin\frac{1}{2}\Theta$, we obtain for the scattering amplitudes in the new system

$$\begin{aligned} T_{2\pm2} &= -ikR_0^2\beta(4\pi)^{-\frac{1}{2}}\tfrac{1}{4}\sqrt{\tfrac{3}{2}}[J_2(x)-J_0(x)]e^{\pm2i\phi_R}, \\ T_{20} &= ikR_0^2\beta(4\pi)^{-\frac{1}{2}}\tfrac{1}{4}[3J_2(x)+J_0(x)]. \end{aligned} \tag{25}$$

The angular dependence of these amplitudes is contained in the combinations of Bessel functions (J_2-J_0) and $(3J_2+J_0)$, and these factors are shown in fig. 14 as functions of x. Beyond $x = 4$ they have very similar behaviour, and both converge asymptotically to the function $4(2\pi x)^{-\frac{1}{2}} \sin(x+\frac{1}{4}\pi)$. However, over the range shown in fig. 14 there remains a definite gap between the values of x at which the two functions attain the value zero. These zero gaps have a special significance, in that they correspond to regions of discontinuous behaviour for the phase parameter δ_0 and to

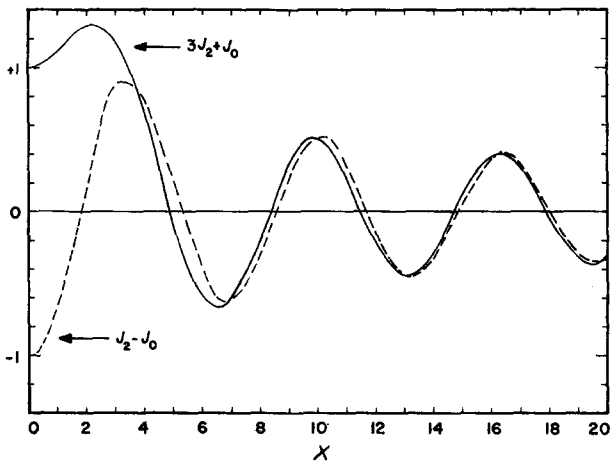

Fig. 14. Functions $3J_2(x)+J_0(x)$(solid curve) and $J_2(x)-J_0(x)$(dashed curve).

regions of rapid variation for the amplitude parameter a_0 and the reaction-plane gamma-ray yield Y, as discussed in sect. 4 of this paper.

References

1) J. G. Cramer, Jr. and W. W. Eidson, Nuclear Physics **55** (1964) 593
2) W. W. Eidson, J. G. Cramer, Jr., R. D. Bent and D. E. Blatchley, Bull. Am. Phys. Soc. **8** (1963) 11;
D. E. Blatchley, R. D. Bent, and J. G. Cramer, Jr., Bull. Am. Phys. Soc. **8** (1963) 47
3) W. W. Eidson and J. G. Cramer, Jr., Bull. Am. Phys. Soc. **8** (1963) 303
4) R. Scherr and W. F. Hornyak, Bull. Am. Phys. Soc. **1** (1956) 197
5) K. K. McDaniels, D. L. Hendrie, R. H. Bassel, and G. R. Satchler, Phys. Lett. **1** (1962) 295
6) F. H. Schmidt, R. E. Brown, J. B. Gerhart, and W. A. Kolasinski, to be published
7) W. W. Eidson and R. D. Bent, Phys. Rev. **128** (1962) 1312
8) W. W. Eidson and R. D. Bent, Phys. Rev. **127** (1962) 913
9) R. H. Moore and R. K. Ziegler, Los Alamos Sci. Lab. Report LA-2367 (1959), unpublished
10) M. E. Rose, Phys. Rev. **91** (1953) 610
11) D. J. Rowe, G. L. Salmon, and A. B. Clegg, Nucl. Instr. **12** (1961) 353
12) R. D. Evans, The Atomic Nucleus (McGraw-Hill, New York, 1955) p. 774
13) J. G. Cramer Jr. and W. W. Eidson, Bull. Am. Phys. Soc. **8** (1963) 317
14) J. S. Blair and L. Wilets, Phys. Rev. **121** (1961) 1493
15) G. B. Schook, Phys. Rev. **114** (1959) 310
16) F. D. Seward, Phys. Rev. **114** (1959) 514

17) H. S. Adams and N. M. Hintz, Univ. of Minnesota Lin. Acc. Report (1959), unpublished
18) H. A. Lackner, G. F. Dell and H. J. Hausman, Phys. Rev. **114** (1959) 560;
H. J. Hausman, G. F. Dell and H. F. Bowsher, Phys. Rev. **118** (1960) 1237;
H. F. Bowsher, G. F. Dell and H. J. Hausman, Phys. Rev. **121** (1961) 1504
19) H. Yoshiki, Phys. Rev. **117** (1960) 773
20) H. Taketani and W. P. Alford, Nuclear Physics **32** (1962) 430
21) H. Halabei, N. Martalogu, J. Frantz, M. Ivascu, N. Scintei, A. Berinde and I. Neamu, Phys. Rev. **126** (1962) 2174
22) H. Halubei, N. Martalogu, M. Ivascu, N. Scintei, A. Berinde, I. Neamu and J. Francz, Phys. Rev. **132** (1963) 796
23) Y. Nagahara, N. Yamamuro, R. Kajikawa, N. Takano, S. Kobayashi and K. Matsuda, Proc. of Padua Conf. on Direct Reactions and Nuclear Reaction Mechanisms (Gordon and Breach, N.Y. 1962)
24) D. E. Blatchley, Ph. D. Thesis, Indiana University (1963), unpublished
25) S. T. Butler, N. Austern, and C. Pearson, Phys. Rev. **112** (1958) 1227
26) G. R. Satchler, Proc. Phys. Soc. (London) **68** (1955) 1306
27) A. B. Clegg and G. R. Satchler, Nuclear Physics **27** (1961) 431
28) S. I. Drozdov, JETP **1** (1955) 588, 591
29) J. S. Blair, Phys. Rev. **115** (1959) 928
30) G. R. Satchler, Nuclear Physics **18** (1960) 289
31) J. G. Wills and J. G. Cramer, Jr., Proc. of the Conf. on Nuclear spectroscopy with Direct Reactions (I) Contributed Papers, Argonne National Laboratory Report ANL-6848 (1964); and to be published
32) G. R. Satchler, private communication
33) M. K. Banerjee and C. A. Levinson, Ann. of Phys. **2** (1957) 499
34) R. M. Drisko, G. R. Satchler and R. H. Bassel, Phys. Lett. **5** (1963) 347
35) J. M. Blatt and V. F. Weisskopf, Theoretical nuclear physics (J. Wiley and Sons, New York, 1952)
36) L. C. Biedenharn, Nuclear spectroscopy, Part B, ed. by F. Ajzenberg-Selove (Academic Press, New York, 1960)
37) S. Devons and L. J. B. Goldfarb, Handbuch der Physik XLII (Springer-Verlag, Berlin, 1957)
38) L. Wolfenstein, Phys. Rev. **82** (1951) 690
39) W. Hauser and H. Feshbach, Phys. Rev. **87** (1952) 366
40) E. Sheldon, Helv. Phys. Acta **34** (1961) 803
41) E. Sheldon, Nuclear Physics **37** (1962) 302
42) G. R. Satchler, Phys. Rev. **94** (1954) 1304
43) H. Feshbach, Ann. of Phys. **19** (1962) 287, **5** (1958) 357
44) N. Austern, Proc. of Gatlinburg Conf. on States of the Compound Nucleus (1963)
45) M. E. Rose, Elementary theory of angular momentum (J. Wiley & Sons, New York, 1957)
46) A. Bohr, Nuclear Physics **10** (1959) 486